Chapter 2

Spin injection concepts

2.1 Spin injection due to charge current

2.1.1 Electrical properties of ferromagnetic metals

In contrast to paramagnetic materials, where the electron spins interact only with an external magnetic field, the spins in ferromagnetic materials interact strongly with each other, each of them trying to align the others in its own direction. Even in the absence of an applied field this effect, called exchange interaction, creates a certain degree of order which is the cause of a non-zero average magnetic moment in zero field, the main difference between paramagnetism and ferromagnetism. The collective ordering of the electron spins creates a macroscopic magnetic moment, i.e. magnetization. The Stoner model assumes that the density of states (DOS) for the majority (those antiparallel to the local magnetization) and minority electrons is often nearly identical, but the states are shifted in energy with respect to each other by the exchange energy. This implies that the DOS at the Fermi energy becomes different for the two spin sub-bands, as it is shown in Fig. 2.1. The electrons at the Fermi energy are those responsible for electric transport; in metallic ferromagnets, such as the transition metals, Ni, Fe, Co, the conducting electrons are spin polarized, and a charge current is accompanied by a current of spins.

The electrical transport in metallic ferromagnets, assuming weak spin-flip scattering processes can be described by a two-channel resistor model, according to which currents of two spin populations flow in parallel. As a result, the total current can be expressed as two parallel electron currents, which are in turn limited by resistors in series that represent bulk scattering. Given this, in ferromagnets the conductivities for the spin-up ($\uparrow$) and down ($\downarrow$) channels are different, $\sigma_{\uparrow,\downarrow} = e^2 N_{\uparrow,\downarrow} D_{\uparrow,\downarrow}$ (Einstein relation) [1]. Here $N_{\uparrow,\downarrow}$ is the spin dependent DOS at the Fermi energy, $D_{\uparrow,\downarrow}$ the spin dependent diffusion constant. Throughout this thesis our notation is $\uparrow$ for the majority

spin direction and $\downarrow$ for the minority spin direction. The current flowing in a bulk ferromagnet is spin polarized, with polarization defined as

$$\alpha_F \equiv \frac{j_\uparrow - j_\downarrow}{j_\uparrow + j_\downarrow} = \frac{\sigma_\uparrow - \sigma_\downarrow}{\sigma_\uparrow + \sigma_\downarrow} \tag{2.1}$$

where $j_{\uparrow\downarrow}$ are the spin-up and spin-down current densities. In transition metal ferromagnets the magnitude of α_F is in the range of 0.3 to 0.7.

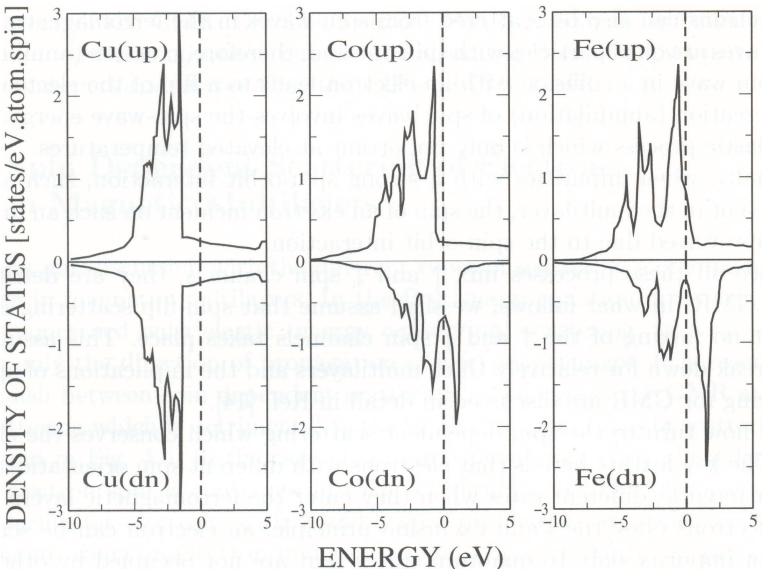

Figure 2.1: *Calculated densities of states of copper, cobalt and iron. Dashed line denotes the position of the Fermi level [2].*

2.1.2 The basics of spin transport

The electron transport through a diffusive channel is a result of a difference in the electrochemical potential of two connected electron reservoirs [3]. The electrochemical potential μ_{ch} is by definition the energy needed to add one electron to the system, usually set to zero at the Fermi energy (this convention is adapted throughout this text), and accounts for the kinetic energy of the electrons. In the linear response regime ($|eV| < kT$), the electrochemical potential equals the excess electron particle density n divided by the density of states at the Fermi energy, $\mu_{ch} = n/N(E_F)$. In addition an electron may also have a potential energy, e.g. due to the presence of an electric field $\mathbf{E}$. The additional potential energy for a reservoir at potential V should be added to μ_{ch} in order to obtain the electrochemical potential $\mu = \mu_{ch} - eV$, where e denotes the absolute value of the electron charge.

The theory of spin transport is focused on the diffusive transport regime, which applies when the electron mean free path (l_e) is shorter than the

device dimensions. In this limit the physics can be described by Boltzmann or diffusion equations. Valet and Fert [4] have analyzed the GMR effect in magnetic multilayers using a spin polarized linear Boltzmann equation to derive a diffusion equation including spin-flip scattering. For vanishing spin-flip scattering it reduces to the two-current model (spin-up and spin-down) pioneered by Mott [5]. This idea was followed by Fert and Campbell to describe the transport properties of Ni, Fe and Co based alloys [6]. Van Son et al. [7] have extended the model to describe transport through transparent ferromagnetic metal-nonmagnetic metal interfaces. An alternative model, based on thermodynamic considerations, has been put forward and applied by Johnson and Silsbee [8].

In the following we discuss spin transport in a diffusive normal (paramagnetic) metal in the linear response regime using the two-current model. Assuming the spin life time is much longer than the momentum relaxation time, the two spin species can be treated as separate, weakly connected, ensembles with their own electrochemical potentials assigned to them. Ohm's law applies for both spin species separately

$$j_\uparrow = \frac{\sigma_\uparrow}{e}\frac{\partial \mu_\uparrow}{\partial x}\ ; \quad j_\downarrow = \frac{\sigma_\downarrow}{e}\frac{\partial \mu_\downarrow}{\partial x} \tag{2.2}$$

The next step is the introduction of spin-flip processes, described by a spin-flip time $\tau_{\uparrow\downarrow}$ for the average time to flip an spin-up to a spin-down and $\tau_{\downarrow\uparrow}$ for the reverse process. Particle conservation requires:

$$\frac{1}{e}\nabla j_\uparrow = -\frac{n_\uparrow}{\tau_{\uparrow\downarrow}} + \frac{n_\downarrow}{\tau_{\downarrow\uparrow}}\ ; \quad \frac{1}{e}\nabla j_\downarrow = +\frac{n_\uparrow}{\tau_{\uparrow\downarrow}} - \frac{n_\downarrow}{\tau_{\downarrow\uparrow}} \tag{2.3}$$

with $n_\uparrow$ and $n_\downarrow$ being the excess particle densities for each spin. Detailed balance imposes that $N_\uparrow/\tau_{\uparrow\downarrow} = N_\downarrow/\tau_{\downarrow\uparrow}$, so that in equilibrium no net spin scattering takes place. As pointed out already, usually these spin-flip times are larger than the momentum scattering time $\tau_e = l_e/v_F$. The transport can then be described in terms of the parallel diffusion of the two spin species, where the densities are controlled by spin-flip processes. It should be noted, however, that in particular in ferromagnets (e.g. permalloy [9–11]) the spin-flip times may become comparable to the momentum scattering time. Combining the above equations and using the Einstein relation the effect of the spin-flip processes can be described by the following diffusion equation (assuming diffusion in one dimension only):

$$D\frac{\partial^2(\mu_\uparrow - \mu_\downarrow)}{\partial x^2} = \frac{(\mu_\uparrow - \mu_\downarrow)}{\tau_{sf}}, \tag{2.4}$$

where $D = D_\uparrow D_\downarrow (N_\uparrow + N_\downarrow)/(N_\uparrow D_\uparrow + N_\downarrow D_\downarrow)$ is the spin averaged diffusion constant, and the spin relaxation time τ_{sf} is given by: $1/\tau_{sf} = 1/\tau_{\uparrow\downarrow} + 1/\tau_{\downarrow\uparrow}$.

Note that τ_{sf} represents the timescale over which the non-equilibrium spin accumulation $(\mu_\uparrow - \mu_\downarrow)$ decays and therefore is equal to the spin lattice relaxation time T_1 used in the Bloch equations: $\tau_{sf} = T_1 = T_2$ [12]. Using the requirement of (charge) current conservation, the general solution of Eq. 2.4 for a ferromagnetic or nonmagnetic wire is now given by:

$$\mu_\uparrow = A + Bx + \frac{C}{\sigma_\uparrow} exp(-x/\lambda_{sf}) + \frac{D}{\sigma_\uparrow} exp(x/\lambda_{sf}) \quad (2.5)$$

$$\mu_\downarrow = A + Bx - \frac{C}{\sigma_\downarrow} exp(-x/\lambda_{sf}) - \frac{D}{\sigma_\downarrow} exp(x/\lambda_{sf}) \ , \quad (2.6)$$

where we have introduced the spin relaxation length $\lambda_{sf} = \sqrt{D\tau_{sf}}$. The coefficients A,B,C, and D are determined by the boundary conditions imposed at the junctions where the wires are coupled to other wires. In the absence of interface resistances and spin-flip scattering at the interfaces, the boundary conditions are: 1) continuity of $\mu_\uparrow$, $\mu_\downarrow$ at the interface, and 2) conservation of spin-up and spin-down currents $j_\uparrow$, $j_\downarrow$ across the interface. The non-equilibrium spin accumulation can relax due to spin-flip scattering by spin-orbit interaction and magnetic impurities. In metals the spin relaxation is described by the so called Elliott-Yafet mechanism [13, 14]. In this mechanism the electron spin relaxation is explained in terms of spin-orbit coupling in combination with momentum scattering by impurities (at low T) and phonons (at high T).

2.1.3 The ferromagnet/normal-metal interface

In order to transfer the magnetization from a ferromagnet (F) into a normal-metal (N), a charge current is passed through the F/N interface. As discussed above, the conductivities for the two spin species are different in ferromagnets and the channel with the highest conductance carries more current than the other. On the other side, in the non-magnetic metal, the conductivities are equal. Therefore at the interface between the two metals, a conversion of the excess spins occurs, resulting in a spin accumulation $(\mu_\uparrow - \mu_\downarrow)$ that decays into both metals over the spatial distances λ_N (spin-flip diffusion length in normal-metal) and λ_F (spin-flip diffusion length in ferromagnet), see Fig. 2.2. The interface plays a central role because it contributes with extra resistance (spin dependent or independent) to the total channel resistance.

The transparent F/N interface. Since the discovery of GMR, the electron charge and spin transport properties across the transparent F/N interface have attracted considerable attention. By solving the diffusion equation with the appropriate boundary conditions, one finds that the po-

larization of the current across the interface is given by

$$\alpha = \frac{j_\uparrow - j_\downarrow}{j_\uparrow + j_\downarrow} = \alpha_F \frac{1}{1 + (1 - \alpha_F^2)\frac{\sigma_F \lambda_N}{\sigma_N \lambda_F}} \tag{2.7}$$

where σ_N and σ_F are the conductivities of N and F. Note that the amount of spin current injected through the F/N interface is different than the bulk polarization (α_F) of F. The position dependence of the electrochemical potentials is drawn in Fig. 2.2. Although $\mu_\uparrow$ and $\mu_\downarrow$ are continuous at the interface, $\mu_0 = \alpha\mu_\uparrow + (1 - \alpha)\mu_\downarrow$ is not (μ_0 is defined as the value that electrochemical potential would have without a nonequilibrium current distribution). Thus, the current conversion process in N and F gives rise to an additional voltage drop ($\Delta\mu$). The spin-coupled interface resistance is then given by [15]

$$R_s = \frac{\Delta\mu}{ej} = \alpha_F^2 \frac{\lambda_N \sigma_N^{-1}}{1 + (1 - \alpha_F^2)\frac{\sigma_F \lambda_N}{\sigma_N \lambda_F}} \ . \tag{2.8}$$

The above equations show that the magnitude of the polarization of the current and the spin-coupled resistance is essentially limited by ratio of $\sigma_N^{-1}\lambda_N$ and $\sigma_F^{-1}\lambda_F$. Since the condition $\lambda_F \ll \lambda_N$ holds in almost all cases for metallic systems, this implies that the spin diffusion length in F is the limiting factor to obtain a large polarization. This problem becomes progressively worse, when (high conductivity) metallic ferromagnets are used to inject spin polarized electrons into (low conductivity) semiconductors and has become known as "conductivity mismatch" [16, 17]. Another way to look at it is that the ferromagnetic metal behaves as a very effective spin reservoir because once the electron is diffused (back) into the ferromagnetic metal its spin is flipped very fast. The proximity of the ferromagnetic metal disturbs therefore a non-equilibrium spin population present inside the nonmagnetic metal. The transparent contact is nevertheless the injection method pursued by Johnson and Silsbee (1985) in their seminal experiment, obtaining spin signals in the pV range, and by Jedema et al. (2001), with μV signals.

The tunnel barrier F/I/N interface. A way to increase the efficiency of spin injection is to introduce a spin dependent interface with a resistance much higher than the spin independent resistance [17, 18]. Experimentally this is done by inserting a thin insulating layer between F and N, creating a tunnel barrier for the electrons. Also, the high spin dependent resistance causes the electrons, once injected, to have a negligible probability to lose their spin information by returning back into the ferromagnet. The tunneling spin polarization for a F/I/N tunnel barrier junction is defined as

$$P \equiv \frac{g^\uparrow - g^\downarrow}{g^\uparrow + g^\downarrow} \tag{2.9}$$

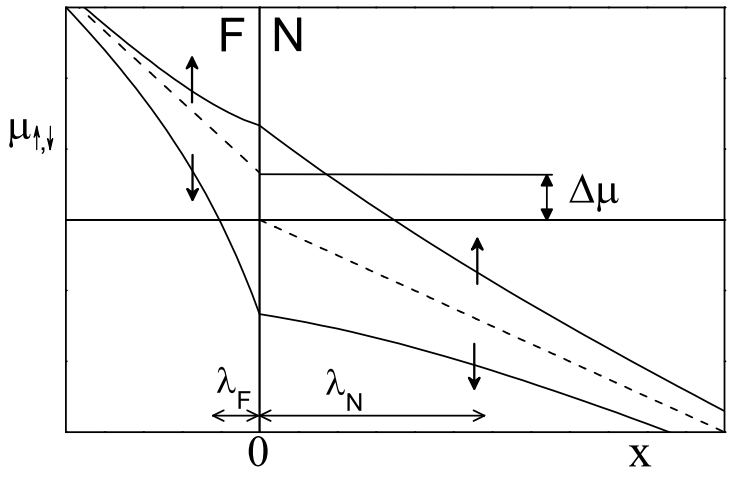

Figure 2.2: *Spatial variation of the electrochemical potentials for spin-up and spin-down electrons with a current flowing through an F/N interface. The dashed lines represent μ_0 (see text). The spin diffusion lengths λ_N, λ_F characterize the decay of spin accumulation $\Delta\mu$ away from the interface into N and F regions [15]. The figure corresponds to $\lambda_N = 5\lambda_F$.*

where $g^{\uparrow}(g^{\downarrow})$ is spin-up (spin-down) conductance.

In tunneling regime the technological interest is monopolized by F/I/F magnetic tunnel junction (MTJ) structure. In this system the two ferromagnetic electrodes are separated by a thin insulating layer, and the resistance depends on the relative orientation of the electrodes' magnetization, i.e. tunneling magnetoresistance (TMR). Julliere (1975) [19] formulated a model for the change of conductance G (1/resistance) between the parallel ($\uparrow\uparrow$) and antiparallel ($\uparrow\downarrow$) magnetization in the two F electrodes.

$$TMR \equiv \frac{G_{\uparrow\uparrow} - G_{\uparrow\downarrow}}{G_{\uparrow\downarrow}} = \frac{2P_1P_2}{1 - P_1P_2} \tag{2.10}$$

where the polarization $P = (N_{\uparrow} - N_{\downarrow})/(N_{\uparrow} + N_{\downarrow})$ is expressed in terms of spin DOS [20]. The discovery of large room-temperature TMR [21] has increased interest in the study of MTJs, with focus on magnetic random-access memory devices [22].

2.1.4 Bloch equations

The spin accumulation in N can be manipulated in two ways. First, via the magnetization direction of the F electrodes, source and detector. Second, with a transverse applied magnetic field which causes precession of the spin accumulation around the field direction, i.e. the Hanle effect. When

the ferromagnets' magnetization vectors and spin accumulations are non-collinear (neither parallel nor antiparallel) to each other, the two-current model cannot be used anymore. The concept of up and down spin states must be replaced by a representation in terms of $\hat{\sigma}_x$, $\hat{\sigma}_y$ and $\hat{\sigma}_z$ operators [23]. The spin dependent chemical potentials $(\mu_\uparrow, \mu_\downarrow)$ are replaced by a spin dependent chemical potential in the three orthogonal directions (μ_x, μ_y, μ_z).

In the presence of the transverse applied field (in the z-direction) and assuming 1-dimensional diffusion along the x-direction, the response of the spin accumulation can be described by the Bloch equations

$$\frac{\partial \mu_x}{dt} = \gamma B \mu_y - \frac{\mu_x}{\tau_{sf}} + D\frac{\partial^2 \mu_x}{\partial x^2} , \tag{2.11}$$

$$\frac{\partial \mu_y}{dt} = -\gamma B \mu_x - \frac{\mu_y}{\tau_{sf}} + D\frac{\partial^2 \mu_y}{\partial x^2} , \tag{2.12}$$

$$\frac{\partial \mu_z}{dt} = -\frac{\mu_z}{\tau_{sf}} + D\frac{\partial^2 \mu_z}{\partial x^2} . \tag{2.13}$$

where $\gamma = g\mu_b/\hbar$ is gyromagnetic ratio, g is the Lande factor and $\mu_b = e\hbar/2m_e$ is the Bohr magneton.
In a metal, and in zero field, there is no distinction between the longitudinal (spin lattice) relaxation time T_1 and the transverse (dephasing) relaxation time T_2, thus we will consider them equal. This set of equations can also be used in the case of ac spin injection experiment (chapter 7), to describe the dynamics of the spin accumulation into N.

2.2 Spin injection due to magnetization precession

So far the discussion has focused on stationary magnetic states (dc regime). In the following we concentrate on spin currents induced by magnetization precession, the so-called spin pumping effect. Moreover, to link this with the stationary case we first discuss the spin transfer torque effect.

2.2.1 Spin transfer torque effect

Slonczewski [24] and Berger [25] predicted that angular momentum is transferred from spin polarized currents to the magnetization of the ferromagnets when charge currents are sent trough F1/N/F2 spin valves with non-collinear magnetizations. This can excite and even switch the magnetization direction of the F2 (here, F2 was assumed to be the softer ferromagnet), see Fig. 2.3. Experiments with pillar-type structures [26–29] confirmed these predictions.

Spin transfer induced magnetization dynamics is a consequence of the spin transport at the N/F interface. The basic process is described in a picture, where an electron is arriving from N with spin-up state $|\uparrow\rangle$ at the N/F interface. This is basically a scattering problem, where the spin components of the incoming electron can be reflected back into N, or can be transmitted into F. We assume that the F is halfmetallic (i.e. the interface is transparent only to the majority spins) and has a magnetization direction in the x-positive axis. This means that at the Fermi energy there are only spin states available in the positive x-direction. In the coordinate system of the ferromagnetic magnetization the incoming spin-up electron is not a eigen state but a linear combination of right $|\rightarrow\rangle$ and left $|\leftarrow\rangle$ polarized spin states. Since no $|\leftarrow\rangle$ states exist in F, this component cannot enter and is reflected. On the other hand the $|\rightarrow\rangle$ component continues into the F. Consequently, both of the outgoing spin states (transmitted and reflected) lie along the x axis, while the incoming spin state is perpendicular to the magnetization. Due to conservation law of angular momentum results that the spin component perpendicular to the magnetization must be absorbed by the F. Thus an angular momentum is transferred to F. Therefore a torque (T) acts on the F which tends to rotate the magnetization direction as shown in Fig. 2.3.

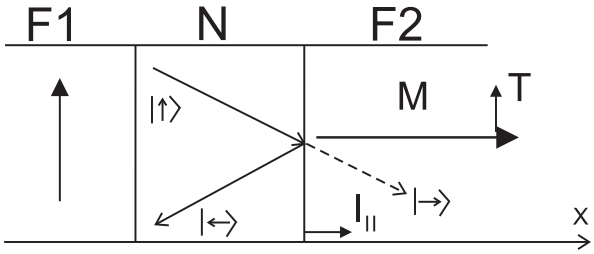

Figure 2.3: *Schematic of spin transfer torque exerted by a spin current. The spin angular momentum is absorbed by the ferromagnet, generating an effective torque on the magnetization [30].*

Some additional points need to be considered in the case of transition metal ferromagnets like Ni, Fe, Co, which are not fully polarized. As discussed above the electron transport in these metals is diffusive and both spin channels conduct. Since minority electrons from N can now enter F, a transverse spin can penetrate F in principle. However, because of the ferromagnetic exchange interaction, the energy of the spin components parallel and antiparallel to the magnetization M will be different. The corresponding precessional motion of the spin direction around the direction of M depends on wave vectors ($k_F^{\uparrow}$, $k_F^{\downarrow}$), which leads to destructive interference of the spin components perpendicular to M. The distance at which the transverse component of the spin current disappears is called the ferromagnetic

coherence length, $\pi/|k_F^{\uparrow} - k_F^{\downarrow}|$ [30]. In transition metals is usually a few Å, much smaller than mean free path or spin diffusion length.

A general description of spin transport in N/F hybrid systems within the framework of magnetoelectronic circuit theory was given by Brataas et al. [31, 32]. To describe the interaction of the electrons spin with the magnetization at the N/F interface, a "spin mixing" conductance $g^{\uparrow\downarrow}$ was introduced, which can be expressed in terms of the spin dependent reflection coefficients at the interface. It was found that the magnitude of the spin torque is directly proportional to the spin mixing conductance [32]. Physically, $g^{\uparrow\downarrow}$ is a material parameter that describes how a given spin accumulation transmits a torque to the magnetization at a certain interface. $g^{\uparrow\downarrow}$ was evaluated for different interfaces by first principle band calculations by Xia et al. [33] and compared with experiments provided that the interface $g^{\uparrow\downarrow}$ is renormalized to include bulk material scattering. For most ferromagnets (except ferromagnetic insulators) the imaginary part of the $g^{\uparrow\downarrow}$ is very small, thus will be disregarded it the following. For metallic structures, the band-structures calculations show that real part of $g^{\uparrow\downarrow}$ is close to Sharvin conductance of the N [34].

2.2.2 Spin pumping effect

Introduction. It is natural to expect that if a spin current can induce magnetization motion, then the reciprocal or inverse process may also be possible: a moving magnetization in a ferromagnet (F) can emit a spin current into an adjacent conductor.

The transfer of spin angular momentum by the precessing magnetization of F in contact with N was described by Tserkovnyak et al. [35] and the effect is called "spin pumping". They used the formalism of parametric charge pumping [36] developed in the context of mesoscopic scattering problems in order to show that the time-dependent magnetization induces spin emission.

A simplified picture of the process is given in Fig. 2.4. Let us first consider a F/N junction at equilibrium. In F, there is a larger population of spins that are in the direction of magnetization than are antiparallel. If the magnetization direction is suddenly switched, then the bands shift in energy instantaneously. However, in order to go back to the equilibrium situation there has to be spin transfer from one spin population to another one (spin relaxation). If F is in contact with N this transfer of spins can go via N. Thus the spin relaxation process for F is modified when it is in contact with an adjacent N, and depends on the spin relaxation properties on N. In the main, an oscillating spin current is emitted into N when the magnetization is switched back and forth by an oscillating magnetic field. A way to periodically change magnetization direction is to put F into ferromagnetic resonance (FMR), where circular precession of the magnetization can be

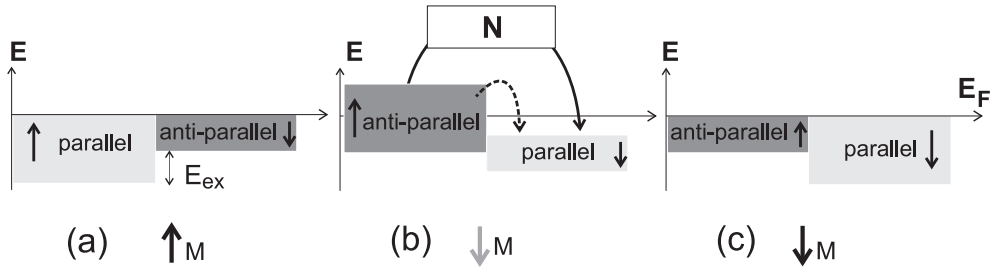

Figure 2.4: *(a) Population of spin-up and spin-down bands in equilibrium. (b) Suddenly reverse the magnetization direction. The arrows denoted spin flow from one spin population to another one. (c) Equilibrium situation again but with magnetization in opposite direction. [Adapted from ref. [37]]*

resonantly excited by a small applied rf magnetic field. This is described in a more detail in section 2.3.

Spin currents at the interface. Assuming the FMR state, Tserkovnyak et al. [35] have calculated the spin pumped current using a scattering matrix approach based on the microscopic details of the interface,

$$\boldsymbol{I}_s^{pump} = \frac{\hbar}{4\pi} g^{\uparrow\downarrow} \mathbf{m} \times \frac{d\mathbf{m}}{dt} \,. \tag{2.14}$$

$g^{\uparrow\downarrow}$ is the real part of mixing conductance. This equation shows that the spin current which goes into N is perpendicular both to the magnetization direction $\mathbf{m}$ and to the change of $\mathbf{m}$ with time. This current has ac and dc components, however in the limit $\omega\tau_N \gg 1$ (see later discussion), the time averaged pumping current reads $|\langle \boldsymbol{I}_s^{pump} \rangle_t| = I_{dc} = \hbar\omega g^{\uparrow\downarrow} sin^2\theta/4\pi$.
To sum up, the magnetization precession induces an emission of spins oriented transverse to $\mathbf{m}$ into N. Because transport in metals is diffusive, this transverse component is lost everywhere in F, except on the ferromagnetic coherence length, close to the interface. Therefore, it can be transmitted by diffusion of the electrons to N, resulting in a transverse spin current (spin pump current).

Depending on the spin related properties of the N, the spin current emission has two limiting regimes. When the N is a good "spin sink" (in which spins relax fast), the injected spin current is quickly dissipated and this corresponds to a loss of angular momentum and an increase in the effective Gilbert damping of the magnetization precession. This has been observed experimentally in nanopillars structures [38–41]. The total spin current is given by $\boldsymbol{I}_s^{pump}$.

The opposite regime is when the spin-flip relaxation rate is smaller than the spin injection rate. In this case a spin accumulation $\boldsymbol{\mu}_s^N$ builds up in

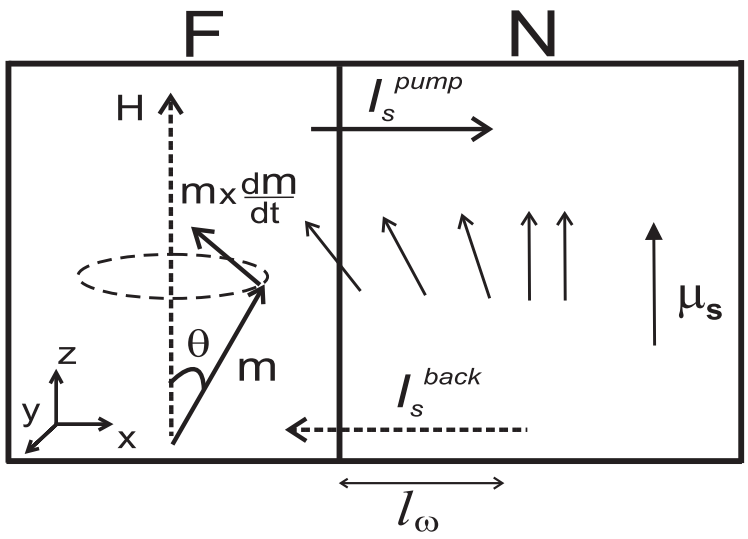

Figure 2.5: *The F/N structure in which the resonant precession of the magnetization direction* $\mathbf{m}$ *pumps a spin current* $\boldsymbol{I}_s^{pump}$ *into N. The spin pumping builds up a spin accumulation* $\boldsymbol{\mu}_s^N$ *in N that drives a spin current* $\boldsymbol{I}_s^{back}$ *back into the F. The component of the* $\boldsymbol{I}_s^{back}$ *parallel to* $\mathbf{m}$ *can enter into F. Since the interface and the bulk conductances of F are spin dependent, this can result in a dc voltage across the interface.*

the normal-metal (Fig. 2.5). The spin accumulation can diffuse away from the interface, but can also diffuse back into the F. This back flow current is given by

$$\boldsymbol{I}_s^{back} = \frac{g_{\uparrow\downarrow}}{2\pi N}[\boldsymbol{\mu}_s^N - \mathbf{m}(\mathbf{m}\cdot\boldsymbol{\mu}_s^N)] \,, \tag{2.15}$$

where N is the one-spin density of states. The total spin current in this case is $\boldsymbol{I}_s^F = \boldsymbol{I}_s^{pump} + \boldsymbol{I}_s^{back}$.

Spin battery. A spin battery operated by FMR has been proposed by the Brataas et al. [42] in the limit of weak spin-flip scattering in the F. The spin accumulation in N can be calculated by solving the spin diffusion equation,

$$\frac{\partial \boldsymbol{\mu}_s^N}{\partial t} = D_N \frac{\partial^2 \boldsymbol{\mu}_s^N}{\partial x^2} - \frac{\boldsymbol{\mu}_s^N}{\tau_N} \tag{2.16}$$

where τ_N is the spin-flip time and D_N is the diffusion coefficient in N. We assume that the spin diffusion length in N is much larger than the spin precession length $l_\omega \equiv \sqrt{D_N/\omega}$ (ω is precessional frequency), i.e. $\lambda_N = \sqrt{D_N/\tau_N} \gg l_\omega$, or equivalent by $\omega\tau_N \gg 1$. This means that if the length of N is larger than l_ω, the x, y components of spin accumulation are fully averaged (due to dephasing) and the remaining z component is constant and along the static magnetic field direction [42]. The time averaged spin

accumulation $\langle \boldsymbol{\mu}_s^N \rangle_t = \mu_z^N \mathbf{z}$ in the N close to the interface reads [42]

$$\mu_z^N = \hbar\omega \frac{sin^2\theta}{sin^2\theta + \eta} \,, \tag{2.17}$$

where θ is the precession cone angle and η is a reduction factor determined by the ratio between injection and spin-flip relaxation times.
In principle, this spin accumulation can be measured electrically by using a second ferromagnet as a spin dependent contact, placed at a shorter distance compared to the spin-flip length [42, 43].

Voltage at F/N interface. Importantly, Wang et al. [44] have predicted a more direct way to detect the spin pump effect in which the precessing ferromagnet acts also as the detector. We have to take into account that the spin accumulation $\boldsymbol{\mu}_s^N$ in a diffusive metal drives the spin current $\boldsymbol{I}_s^{back}$ back into the F. The component parallel to $\mathbf{m}$ can enter F. Moreover, since the interface and the bulk conductances of F are spin dependent, this can result in charge accumulation close to the interface and thereby a dc voltage across the interface. The chemical potential difference (voltage) across the interface has been calculated by Wang et al. [44] following the lines of the Brataas et al. [42] model, but including the spin diffusion back into F and spin-relaxation in F. As mentioned above, the relevant length-scale for the averaging of the transverse (x, y) components of the spin current is l_ω. Therefore for a device with dimensions larger than l_ω the spin-up (down) effective conductances $g_\omega^{\uparrow(\downarrow)}$ of the interface are composed of the interface conductances $g^{\uparrow(\downarrow)}$ in series with a conductance of the bulk N over a length scale of l_ω. These relations are given by $g_\omega^{\uparrow(\downarrow)} = g^{\uparrow(\downarrow)}/(1 + g^{\uparrow(\downarrow)}/g_\omega)$ and the mixing conductance $g_\omega^{\uparrow\downarrow} = g^{\uparrow\downarrow}/(1 + g^{\uparrow\downarrow}/g_\omega)$, where $g_\omega = (\sigma_N A)/l_\omega$ (A is the area of the interface). $p_\omega = (g_\omega^\uparrow - g_\omega^\downarrow)/(g_\omega^\uparrow + g_\omega^\downarrow)$ is also introduced.

In the limit of large spin-flip in F and the size of N $\gg \lambda_N$ and for small angle precession ($\theta \to 0$), the chemical potential difference is given by [44]

$$\Delta\mu_0 = \frac{p_\omega g_\omega^{\uparrow\downarrow}}{2(1 + \frac{g_N}{g_F})(1 - p_\omega^2)(g_\omega^\uparrow + g_\omega^\downarrow) + 2g_N} \theta^2 \hbar\omega \,, \tag{2.18}$$

where g_N (g_F) is the conductance of the bulk N (F) over a length scale of λ_N (λ_F). For a thorough review of the above discussion see ref. [44]. In chapter 7 we show that a dc voltage $V_{dc} = \Delta\mu_0/e$ is detected at the F/N interface when the F in ferromagnetic resonance pumps spins into N in combination with spin dependent conductivities of the F.

Interface currents matching. In this section, we describe a simple way to find the voltage (similar to Eq. 2.18) using spin-currents matching at the interface [45]. By writing all the currents involved in the process and matching them at the interface, all components of the spin accumulation at the interface can be determined. It is convenient to transform the equations into a rotating frame of reference in which the uniform magnetization

motion can be formally eliminated, and the unit magnetization vector is $\hat{\mathbf{m}} = (sin\theta, 0, cos\theta)$.
Basically for this problem we have to consider three currents with their components. First, the spin pumping current (Eq. 2.14) is given by

$$I_{s,\perp}^{pump} = g^{\uparrow\downarrow} sin\theta \hbar\omega \ . \tag{2.19}$$

The back flow current consists of a term parallel to $\hat{\mathbf{m}}$ and a term perpendicular to $\hat{\mathbf{m}}$, and it is written in terms of spin accumulation $\boldsymbol{\mu}$ at the interface

$$I_s^{back} = g_F \mu_{\parallel} + g^{\uparrow\downarrow} \mu_{\perp} \ . \tag{2.20}$$

The sum of Eq. 2.19 and 2.20, $I_s^{pump} + I_s^{back} = I_s^F$, is the total spin current on the F side of the interface.
The spin current on the N side of the interface is found by solving the Bloch equations for the spin accumulation in N. From this the current at the interface is given by [46]

$$I_s^N = g_\omega \begin{pmatrix} \mu_x - \mu_y \\ \mu_x + \mu_y \\ \frac{g_N}{g_\omega}\mu_z \end{pmatrix} \tag{2.21}$$

in terms of $\boldsymbol{\mu}$ at the interface. This current has three components. The z component is determined only by the usual spin relaxation process. For the x and y components, two effects are important: precession, which results in mixing of the two components, depending on the time spent in N; and averaging, which reduces the total amplitude of the components. $\boldsymbol{\mu}$ is determined by matching (conservation) the currents at the interface $I_s^N = I_s^F = I_s^{back} + I_s^{pump}$. The dc voltage at the interface is proportional to the projection of $\boldsymbol{\mu}$ onto $\hat{\mathbf{m}}$,

$$V = -p\boldsymbol{\mu} \cdot \hat{\mathbf{m}} \simeq -p\frac{g_\omega}{g_F}\left(1 - \frac{g_N}{g_\omega}\right) \cos\theta \sin^2\theta \hbar\omega \ . \tag{2.22}$$

The simple form of Eq. 2.22 results from the relative independence of the dc voltage on $g^{\uparrow\downarrow}$. Let us compare the different conductances in the problem:

$$\begin{aligned} \frac{g_F}{A} &= \frac{\sigma_F}{\lambda_F} = \frac{6.6 \times 10^6 \Omega^{-1} m^{-1}}{5nm} \simeq 1 \times 10^{15} \frac{1}{\Omega m^2} \\ \frac{g_\omega}{A} &= \frac{\sigma_N}{l_\omega} = \frac{3.1 \times 10^7 \Omega^{-1} m^{-1}}{300nm} \simeq 1 \times 10^{14} \frac{1}{\Omega m^2} \\ \frac{g_N}{A} &= \frac{\sigma_N}{\lambda_N} = \frac{3.1 \times 10^7 \Omega^{-1} m^{-1}}{500nm} \simeq 8 \times 10^{13} \frac{1}{\Omega m^2} \ . \end{aligned} \tag{2.23}$$

According to ref.[33],

$$\frac{g^{\uparrow\downarrow}}{A} \approx 5 \times 10^{14} \frac{1}{\Omega m^2} \ . \tag{2.24}$$

Here F denotes permalloy (Py) with $\sigma_{Py} = 6.6 \times 10^6 \Omega^{-1} m^{-1}$, for comparison Co has $\sigma_{Co} = 4.2 \times 10^6 \Omega^{-1} m^{-1}$ and N denotes Al with $\sigma_{Al} = 3.1 \times 10^7 \Omega^{-1} m^{-1}$, for comparison Cu has $\sigma_{Cu} = 3.5 \times 10^7 \Omega^{-1} m^{-1}$, all at room temperature.

Finally, let's estimate Eqs. 2.18 and 2.22. We assume $\theta \approx 5°$ ($sin^2\theta = 0.01$) and $\omega = 10^{11} s^{-1}$ ($\hbar\omega = 65\mu eV$). First Eq. 2.22, using $p = 0.4$ this equation gives ≈10-20 nV. Second Eq. 2.18, using $p_\omega = 0.06$, $\frac{g^\uparrow}{A} = 0.31 \times 10^{15} \Omega^{-1} m^{-2}$ and $\frac{g^\downarrow}{A} = 0.19 \times 10^{15} \Omega^{-1} m^{-2}$ (from ref. [15]), the voltage is also of the order of 10-20 nV.

2.3 Magnetization dynamics

Part of the classical approach to ferromagnetism is to replace the spins by a classical macro-spin vector $\vec{M}$ magnetization. The time-dependence of the magnetization can be obtained directly by calculating the torque acting on $\vec{M}$ by an effective magnetic field H,

$$\frac{d\vec{M}}{dt} = -\gamma \vec{M} \times \vec{H}, \tag{2.25}$$

where $\gamma = g\mu_b/\hbar$ is gyromagnetic ratio, g is the spectroscopic splitting factor (Lande factor) and $\mu_b = e\hbar/2m_e$ is the Bohr magneton. This equation represents an undamped precession of the magnetization. From experiments actual changes of the magnetization are known to decay in a finite time. The damping is just added as a phenomenological term to Eq. 2.25

$$\frac{d\vec{M}}{dt} = -\gamma \vec{M} \times \left(\vec{H} - \frac{\alpha}{\gamma M_s} \frac{d\vec{M}}{dt} \right) = -\gamma \vec{M} \times \vec{H} + \frac{\alpha}{M_s} \vec{M} \times \frac{d\vec{M}}{dt}, \tag{2.26}$$

where α is the dimensionless Gilbert damping constant, of order 10^{-2} in F thin films. This form of the equation, named Landau-Lifshitz-Gilbert, LLG, is due to Gilbert, which can be derived from an older form of the Landau and Lifshitz equation [47]. This equation is used throughout this thesis to describe the resonant motion of the magnetization in our devices. In the following we solve this equation for a ferromagnetic strip, the relevant case for the experiments described in this thesis.

2.3.1 Ferromagnetic resonance of a ferromagnetic strip

The most commonly used technique for inducing magnetization coherent rotation is ferromagnetic resonance (FMR). FMR is the physical process whereby magnetization is rotated by an rf magnetic field h_{rf}, with angular frequency ω, that is resonant with the magnetization precession frequency in an external magnetic field h_0, oriented perpendicular to h_{rf}.

We consider a thin ferromagnetic strip, single domain with the equilibrium magnetization along x direction and a saturation magnetization M_s as shown in Fig. 2.6. As shown in equation 2.26, in order to account for the torque acting on $\vec{M}$, we have to define the effective field. Taking into account the applied fields, the demagnetization fields and neglecting the uniaxial anisotropy, the components of the effective field inside the strip are $\vec{H} = (h_0 - N_x m_x, -N_y m_y, h_{rf} - N_z m_z)$. Where N_x, N_y and N_z are the demagnetization factors that depend only on the shape of the ferromagnet, the sum of them is equal to 1. Due to large aspect ratio of our strip, N_x can be neglected, then N_y can be approximated by $N_y \approx t/w$ (t and w are the strip's thickness and width). N_z is simply given by $1 - N_y$. Due to the non-zero N_y and N_z factors the magnetization precessional path around the direction of the applied field h_0 is elliptical. Assuming the small angle limit, we simplify the problem by setting the time derivative of $\vec{M}$ along the direction of h_0 equal to zero, $\frac{dM_x}{dt} = 0$ such that $\vec{M}(t) = (M_s, m_y(t), m_z(t))$. If the rf field is sinusoidal, its time-dependence can be expressed by a factor $e^{i\omega t}$, and the same factor can then be inserted into the steady state solution of m_y and m_z. Using all these assumptions and omitting all terms which are higher that linear in α, the equations of motion for the amplitudes are

$$\begin{aligned} i\omega m_y &= \gamma h_{rf} M_s - \gamma m_z (h_0 + N_z) - i\omega\alpha\, m_z \\ i\omega m_z &= \gamma m_y (h_0 + N_y) + i\omega\alpha\, m_y \,. \end{aligned} \tag{2.27}$$

Setting $h_{rf} = 0$ and taking the determinant of above linear equations to be zero, Kittel equation [48] results:

$$\omega_0^2 = \gamma^2 (h_0 + N_y M_s)(h_0 + N_z M_s) \,. \tag{2.28}$$

This equation gives the resonant precessional frequency of the coherent rotation mode (uniform mode) as a function of the external magnetic field. As will be shown, by measuring the applied field dependence of the resonant frequency, one can obtain the parameters N_y, N_z and M_s.
It is convenient to give the solutions for m_y and m_z in terms of the complex susceptibilities χ_y and χ_z, where $\vec{M} = \vec{\chi} h_{rf}$ and $\vec{\chi} = \vec{\chi}\,' + i\vec{\chi}\,''$. The components for m_y are as follows

$$\chi_y' = \frac{\alpha\gamma M_s \omega^2 A}{\left(\omega^2 - \omega_0^2\right)^2 + (\alpha\omega)^2 A^2} \tag{2.29}$$

$$\chi_y'' = \frac{-\gamma M_s \omega (\omega^2 - \omega_0^2)}{\left(\omega^2 - \omega_0^2\right)^2 + (\alpha\omega)^2 A^2} \tag{2.30}$$

and for m_z

$$\chi_z' = \alpha\chi_y' - \frac{\gamma}{\omega}(h_0 + N_y M_s)\chi_y'' \tag{2.31}$$

$$\chi_z'' = \alpha\chi_y'' + \frac{\gamma}{\omega}(h_0 + N_y M_s)\chi_y' \tag{2.32}$$

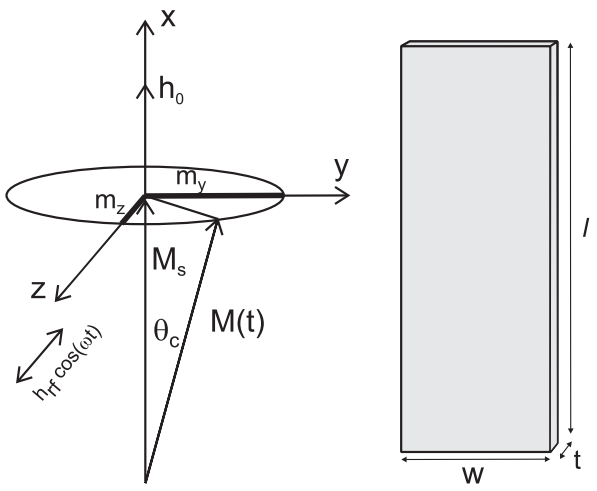

Figure 2.6: *Left, schematic representation of the magnetization $\vec{M}$ precession around the direction of the applied field h_0. Besides this field there is also an rf field $h_{rf}cos\omega t$ which "pushes" the magnetization off-equilibrium and into small amplitude Larmor precession around h_0. On the right side is indicated the geometry of the ferromagnetic strip.*

where $A = \gamma(2h_0 + N_y M_s + N_z M_s)$. As shown in Fig. 2.6 the average

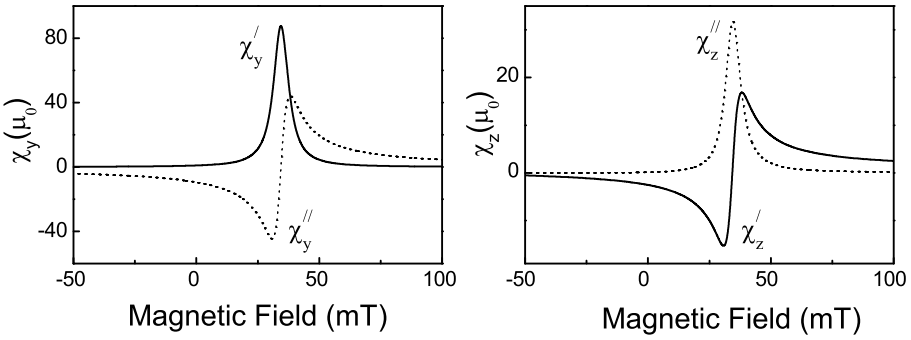

Figure 2.7: *The real and imaginary part of the χ_y and χ_z susceptibilities are calculated at $\omega/2\pi = 10$ GHz, using parameters $M_s = 1$ T, $\alpha = 0.01$ and $\gamma/2\pi = 28$ GHz/T.*

precession cone angle $\theta_c(t)$ can be determined from the relation $\sin^2\theta_c(t) \simeq \theta_c^2(t) = (1/m_s^2)(m_y^2 + m_z^2)$. We found that θ_c^2 can be written as the sum of a time-independent term and terms with time-dependence at twice the driving frequency, $\theta_c^2 = \theta_{dc}^2 + \theta_c^2(2\omega t)$, where $\theta_{dc}^2 = \frac{1}{2}\left(\frac{h_{rf}}{m_s}\right)^2 \left(\chi_y'^2 + \chi_y''^2 + \chi_z'^2 + \chi_z''^2\right)$. Evaluating this angle gives

$$\theta_{dc}^2 = \frac{1}{2}h_{rf}^2 \frac{1 + \left(\frac{\gamma}{\omega}\right)^2 \left(h_0 - (N_x - N_y)\, m_s\right)^2}{\left(\omega^2 - \omega_0^2\right)^2 + (\alpha\omega)^2 A^2} \tag{2.33}$$

Detecting FMR of a single submicron-strip all on-chip is conceptually simple, but experimentally difficult to realize, as it requires a strong microwave driving magnetic field as well as a method for detection. We show in chapter 6, that dc transport measurements, in particular anisotropic magnetoresistance on the ferromagnet are a sensitive probe for microwave induced FMR.

References

[1] Note that in a typical ferromagnetic metal (3d) several bands which have different spin dependent DOS and effective masses contribute to the transport. However, assuming that the elastic scattering time and the inter band scattering times are shorter than the spin flip times (which is usually the case) the transport can be described in terms of spin up and spin down conductivities.

[2] M. Ziese and M. J. Thornton, *Spin Electronics - Lecture Notes in Physics* (Springer, 2001), ISBN 3540418040.

[3] S. Datta, *Electronic transport in mesoscopic systems* (Cambridge University Press, Cambridge, 1995).

[4] T. Valet and A. Fert, Phys. Rev. B **48**, 7099 (1993).

[5] N. F. Mott, Proc. Roy. Soc. **153**, 699 (1936).

[6] E. P. Wohlfarth, *Ferromagnetic Materials* (North Holland, 1982), chap. 9, review article 'Transport properties of ferromagnets', I. A. Campbell, A. Fert, p. 747.

[7] P. C. van Son, H. van Kempen, and P. Wyder, Phys. Rev. Lett. **58**, 2271 (1987).

[8] M. Johnson and R. H. Silsbee, Phys. Rev. B **35**, 4959 (1987).

[9] S. Dubois, L. Piraux, J. George, K. Ounadjela, J. Duvail, and A. Fert, Phys. Rev. B **60**, 477 (1999).

[10] S. D. Steenwyk, S. Y. Hsu, R. Loloee, J. Bass, and W. P. Pratt Jr., J. Mag. Magn. Mater. **170**, L1 (1997).

[11] P. Holody, W. C. Chiang, R. Loloee, J. Bass, W. P. Pratt, Jr., and P. A. Schroeder, Phys. Rev. B **58**, 12230 (1998).

[12] M. Johnson and R. H. Silsbee, Phys. Rev. B **37**, 5312 (1988).

[13] R. J. Elliot, Phys. Rev. **96**, 266 (1954).

[14] Y. Yafet, *Solid State Physics* (Academic, New York, 1963).

[15] F. J. Jedema, Ph.D. thesis, University of Groningen (2002).

[16] G. Schmidt, D. Ferrand, L. W. Molenkamp, A. T. Filip, and B. J. van Wees, Phys. Rev. B **62**, R4790 (2000).

[17] A. T. Filip, B. H. Hoving, F. J. Jedema, B. J. van Wees, B. Dutta, and G. Borghs, Phys. Rev. B **62**, 9996 (2000).

[18] E. I. Rashba, Phys Rev. B Rap. Com. **62**, R16267 (2000).

[19] M. Julliere, Physics Letters **54A**, 225 (1975).

[20] I. Žutić, J. Fabian, and S. D. Sarma, Rev. Mod. Phys. **76**, 323 (2004).

[21] J. S. Moodera, L. R. Kinder, T. M. Wong, and R. Meservey, Phys. Rev. Lett. **74**, 3273 (1995).

[22] S. S. P. Parkin, K. P. Roche, M. G. Samant, P. M. Rice, R. B. Beyers, R. E. Scheuerlein, E. J. O'Sullivan, J. B. S. L. Brown, D. W. Abraham, Y. Lu, et al., J. Appl. Phys. **85**, 5828 (1999).

[23] A. Messiah, *Quantum Mechanics* (Dover Publications, 1999), ISBN 0-487-40924-4.

[24] J. C. Slonczewski, J. Magn. Magn. Mater. **159**,L1 (1996); J.C. Slonczewski, J. Magn. Magn. Mater. **159**,L1 (1996).

[25] L. Berger, Phys. Rev. B **54**, 9533 (1996).

[26] J. Katine, F. Albert, R. Buhrman, E. Myers, and D. Ralph, Phys. Rev. Lett. **84**, 3149 (2000).

[27] J. Grollier, V. Cros, A. Hamzic, J. George, H. Jaffr'es, A. Fert, G. Faini, J. B. Youssef, and H. Legall, Appl. Phys. Lett. **78**, 3663 (2001).

[28] J. Z. Sun, Phys. Rev. B. **62**, 570 (2000).

[29] S. I. Kiselev, J. C. Sankey, I. N. Krivorotov, N. C. Emley, R. J. Schoelkopf, R. A. Buhrman, and D. C. Ralph, Nature **425**, 380 (2003).

[30] A. Brataas, G. E. W. Bauer, and P. Kelly, Physics Reports **427**, 157 (2006).

[31] A. Brataas, Y. V. Nazarov, and G. E. W. Bauer, Phys. Rev. Lett **84**, 2481 (2000).

[32] A. Brataas, G. E. W. Bauer, and P. J. Kelly, Physics Reports **427**, 157 (2006).

[33] K. Xia, P. J. Kelly, G. E. W. Bauer, I. Turek, J. Kudrnovsky, and V. Drchal, Phys. Rev. B **63**, 064407 (2001).

[34] Y. Tserkovnyak, A. Brataas, G. E. Bauer, and B. I. Halperin, Rev. Mod. Phys. **77**, 1375 (2005).

[35] Y. Tserkovnyak, A. Brataas, and G. E. W. Bauer, Phys. Rev. Lett. **88**, 117601 (2002).

[36] M. B*ü*ttiker, H. Thomas, and A. Prtre, Z. Phys. B: Condens. Matter **94**, 133 (1994).

[37] A. Brataas, International Conference on Nanoelectronics, Lancaster University, 4 - 9 January (2003).

[38] S. Mizukami, Y. Ando and T. Miyazaki, J. Magn. Magn. Mater. **226**, 1640 (2001); Phys. Rev. B **66**, 104413, (2002).

[39] R. Urban, G. Woltersdorf, and B. Heinrich, Phys. Rev. Lett. **87**, 217204 (2001).

[40] B. Heinrich, Y. Tserkovnyak, G. Woltersdorf, A. Brataas, R. Urban, and G. E. W. Bauer, Phys. Rev. Lett. **90**, 187601 (2003).

[41] K. Lenz, T. Tolinski, J. Lindner, E. Kosubek, and K. Baberschke, Phys. Rev. B **69**, 144422 (2004).

[42] A. Brataas, Y. Tserkovnyak, G. E. W. Bauer, and B. I. Halperin, Phys. Rev. B **66**, 060404 (2002).

[43] F. J. Jedema, H. B. Heersche, A. T. Filip, J. J. A. Baselmans, and B. J. van Wees, Nature **416**, 713 (2002).

[44] X. Wang, G. E. W. Bauer, B. J. van Wees, A. Brataas, and Y. Tserkovnyak, Phys. Rev. Lett. **97**, 216602 (2006).

[45] S. M. Watts, unpublished.

[46] S. Watts, J. Grollier, C. H. van der Wal, and B. J. van Wees, Phys. Rev. Lett. **96**, 077201 (2006).

[47] W. F. Brown Jr., *Micromagnetics* (Interscience, New York, 1963).

[48] C. Kittel, *Introduction to Solid State Physics, Ch. 16* (John Wiley & Sons, New-York, 7th ed., 1996).